Microelectronics Reliability 129 (2022) 114487

Contents lists available at ScienceDirect

Microelectronics Reliability

journal homepage: www.elsevier.com/locate/microrel

In-situ temperature-dependent characterization of copper through glass via (TGV)

Ke Pan [a,*], Jiefeng Xu [a], Yangyang Lai [a], Seungbae Park [a], Chukwudi Okoro [b], Dhananjay Joshi [b], Scott Pollard [b]

[a] *Department of Mechanical Engineering, Binghamton University, NY, USA*
[b] *Corning Research & Development Corporation, NY, USA*

ARTICLE INFO

Keywords:
TGV
Thermomechanical reliability
Copper protrusion
In-plane deformation
2D DIC

ABSTRACT

Glass has been proposed as a promising material for interposer because of its outstanding material properties. The development of through-glass via (TGV) technology is the most challenging process in the fabrication of glass interposers. This study investigates thermomechanical responses of TGVs induced by thermal loading. Optical profilometry was used to measure the protrusion of copper vias during thermal cycling. The TGV was heated from room temperature (RT) 23 °C to 400 °C and then cooled to RT. The height of an irreversible copper protrusion was recorded at different temperatures. In-plane deformation of the glass caused by thermal mismatch is investigated. Two-dimensional digital image correlation (2D DIC) was applied to measure the in-plane deformation of the glass near the copper via during thermal cycling. The in-plane displacement of the glass near copper vias reached its maximum around 250 °C, then started decreasing because of the copper protrusion and the significant creep of copper material at elevated temperatures. The effect of temperature ramp rate (4 °C/min, 15 °C/min, 30 °C/min, 50 °C/min) on the in-plane deformation of the glass was studied. The in-plane deformation of the glass can be reduced be applying slower ramp rate, because more significant creep occurs in the copper with slower ramp rate which alleviates the CTE mismatch-induced thermal stress at the copper-glass interface. Measurements were conducted to study the creep behavior of the copper via at different temperatures with one hour duration. Each of four TGV samples was heated to a peak temperature, 100 °C, 200 °C, 300 °C, and 400 °C, respectively, and the temperatures were held for 1 h. The glass in-plane displacements were measured by a 2D DIC. Numerical simulations were performed to provide an insight into the thermomechanical behavior of the copper vias and the glass during thermal cycling. The equivalent creep strain of the copper and the maximum principal stress of the glass are presented based on the simulation results.

1. Introduction

As an effective method to realize connections between silicon dies in 2.5D and 3D chip architectures, through-silicon-via (TSV) interconnect technology has been widely applied in many high-end products, such as memory, high-speed logic, and processing applications [1–3]. However, glass has been demonstrated as a next-generation interposer material because of its outstanding material properties, including an adjustable coefficient of thermal expansion (CTE), good surface quality, excellent electrical performance in high-frequency devices, and low thermal conductivity that can help avoid thermal coupling among chips in 2.5D and 3D IC integration [4–6]. Compared with a silicon interposer, a glass interposer can be manufactured with larger panel sizes, finer pitches, and thinner thicknesses, which makes glass a more cost-effective and manufacturable interposer material than silicon [7]. Moreover, a glass wafer can be fabricated from different materials to achieve desired chemical and physical properties for different applications [8].

The manufacture of glass interposers involves forming TGV, copper plating, chemical and mechanical polishing (CMP), dielectric forming, seed deposition, photolithographing, Cu/Au/Ni plating, seed etching, and cover layer forming [6]. Similar with TSVs, the thermal mismatch between copper and glass can cause various reliability issues, such as glass cracking, copper via protrusion, and copper via sliding and delamination [9–11]. Conventionally, an annealing process after the copper plating and CMP will stabilize the microstructure of electroplated copper [12–14], reduce the residue stress in copper vias, and

* Corresponding author.
E-mail address: kpan12@binghamton.edu (K. Pan).

https://doi.org/10.1016/j.microrel.2022.114487
Received 8 July 2021; Received in revised form 16 December 2021; Accepted 13 January 2022
Available online 22 January 2022

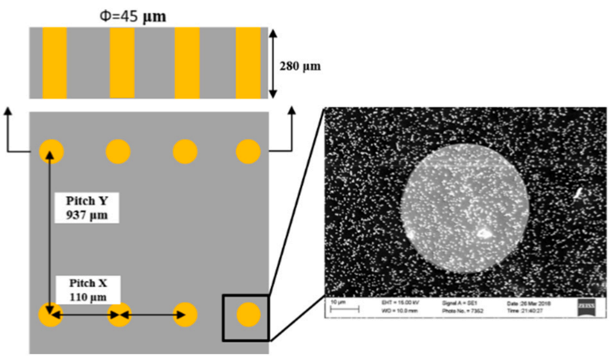

Fig. 1. The schematic of the TGV sample (left), and a patterned copper via (right).

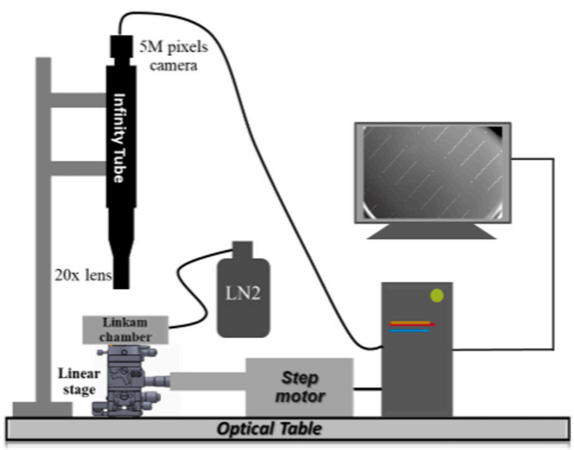

Fig. 2. The schematic of 2D DIC system.

eliminate the protrusion of copper vias induced by the plastic deformation and creep of copper at elevated temperatures [15–19]. The thermomechanical response to the annealing profile was extensively studied by the authors [5,15,20,21]. A thermal profile of 20 min at 400 °C was reported to be the optimal post-plating annealing condition for TSV [20,22]. N. Ranganathan et al. [23] and Xi Liu et al. [24] numerically studied the thermomechanical stress of TSV under thermal loadings. They found that large stress gradients and plastic deformation occurred near the edge of copper vias, which can cause interfacial delamination and dielectric layer cracking. The interfacial reliability of TGV can be improved by strengthening the adhesion between the copper and glass through increased surface area and mechanical locking with the roughened surface [25,26]. Design parameters of the copper via including its diameter, aspect ratio, and pitch have significant effects on the thermomechanical reliability [27–29]. The stress induced by the thermal mismatch can be alleviated by reducing the via diameter and interposer thickness or increasing the pitch of the vias. However, the practical range of the TGV aspect ratio is limited by the process capabilities for copper plating and the deposition of the dielectric and seed layer.

In this paper, temperature-dependent in-situ measurements techniques were used to characterize Cu TGVs. Using white light interferometry technique, Cu protrusion of TGVs were assessed. And a 2D digital image correlation (DIC) technique was used to characterize the in-plane deformation of the glass near the Cu TGVs, for different ramp rates, dwell times and maximum temperatures. Numerical simulation was performed to better understand the overall thermomechanical behavior of the TGV sample during the thermal cycling.

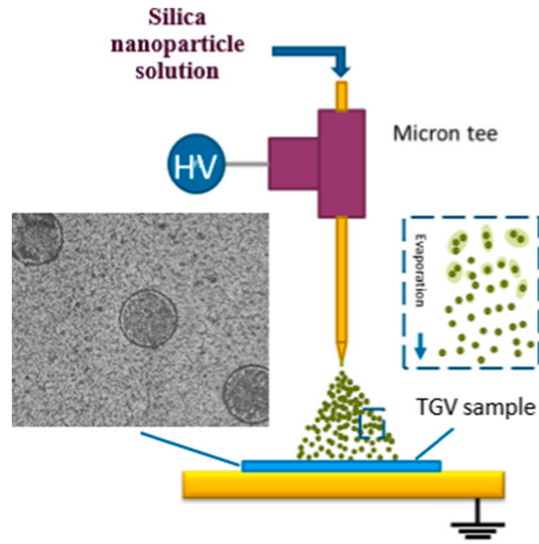

Fig. 3. Electro-spraying sample preparation technique.

2. Experiment setup and TGV sample preparation

The glass substrate used in this work was high purity fused silica (Corning® HPFS® Fused Silica) glass (CTE 0.5 ppm/°C). After holes were made in the glass substrate, titanium (Ti) adhesion layer was deposited, which was followed by copper (Cu) seed layer deposition. Thereafter, by electroplating, the TGVs were fully filled with Cu. The wafer was subsequently subjected to a chemical-mechanical polishing (CMP) step to remove the excess overlaying Cu overburden. The schematic of the structure used in this study is shown in Fig. 1. The via shape is cylindrical with diameter of 45 μm and they are distributed evenly in glass with a different pitch in X and Y direction. The size of the TGV samples is 15 × 8 × 0.28 mm (length × width × thickness).

An optical profiler (Wyko) was used to measure the copper protrusion height at different temperatures. A Linkam chamber is placed on the stage under the objective of the Wyko. This chamber has both low temperature (using liquid nitrogen) and high temperature (hotplate) capability and enables in-situ copper protrusion measurement. The in-plane deformation of the glass during thermal cycling was measured by the 2D DIC. As shown in Fig. 2, the 2D DIC system consists of a 5-million-pixel CCD camera with a 20× magnification lens, a linear stage, and a stepper motor that can adjust the vertical motion of the linear stage. The camera and the step motor were controlled by a program to realize automatic focusing. The Linkam chamber was used to provide the required thermal conditions for the measurement.

In the 2D DIC measurement, the subset size is set as 2 × 2 μm so that in total about ten thousand data point are collected. In addition, the measured surface needs to have a unique feature so that the changes of sample images at different temperatures can be tracked by the DIC algorithm [30–32]. An electro-spraying was employed to generate a random, unique pattern on the top surface of the TGV sample. Silica nanoparticles (100 nm in diameter) were mixed in methanol to form a homogenous solution. High voltage was applied to the solution so that silica nanoparticles were charged and sprayed on the surface of the TGV sample to generate a random pattern (Fig. 3).

3. Experimental results

3.1. Copper via protrusion

Copper via protrusion height at different temperatures was measured using an optical profiler. The field of view of (FOV) o the optical profiler was 320 × 240 μm, which covered 3 copper vias. The height of copper

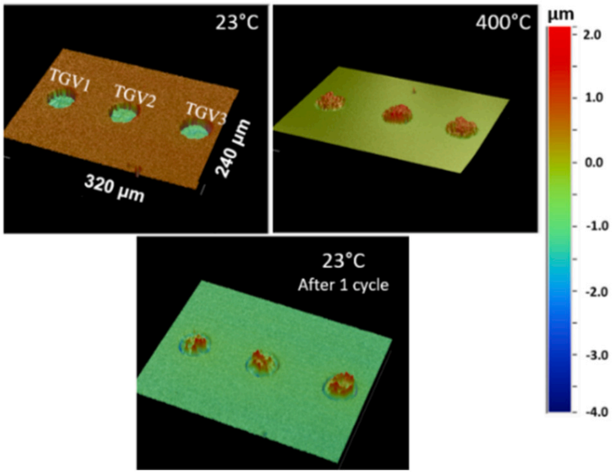

Fig. 4. The copper protrusion height measured by optical profiler.

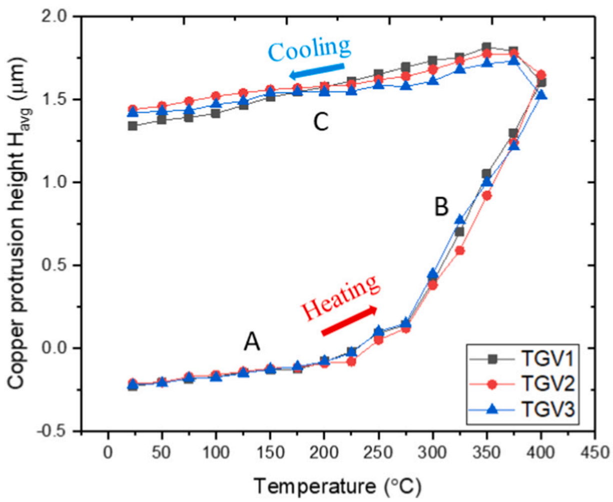

Fig. 5. Protrusion height of copper via at different temperatures.

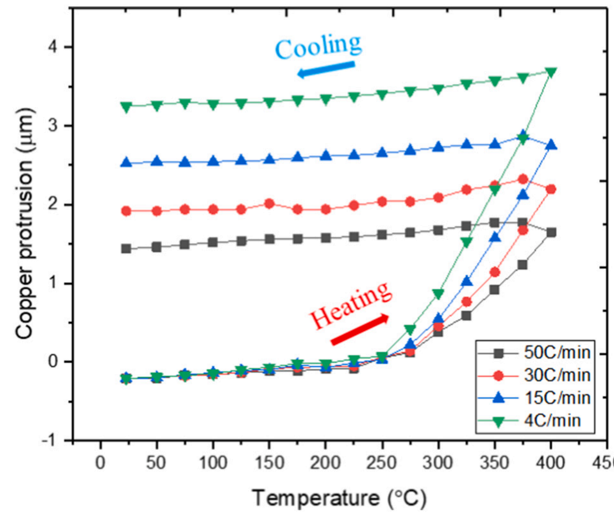

Fig. 6. The copper protrusion results from the experiment and simulation during thermal cycling.

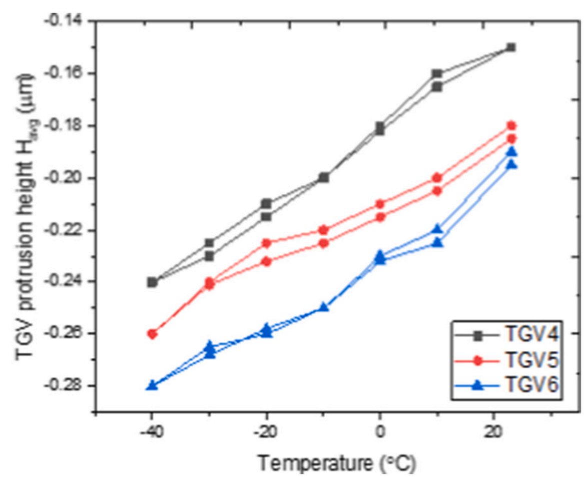

Fig. 7. Protrusion height of copper via at low temperatures.

vias was initially 0.2 μm lower than the top surface of the glass substrate at RT because of the overburden copper removal process. The profile of one thermal cycle increased from RT to 400 °C with a 50 °C/min ramp rate, then cooled to RT by liquid nitrogen (LN2) with the same ramp rate. The average copper protrusion height (H_{avg}) of the 3 vias in the TGV sample was measured after the cycle. Here, H_{avg} represents the difference between the average height of the vias' top surface and the top of the glass substrate that surrounded each via. As shown in Fig. 4, H_{avg} of the 3 vias increased from −0.2 μm to about 1.7 μm when the temperature ramped up to 400 °C. An average irreversible copper protrusion of 1.3 μm remained when the TGV sample was cooled to RT after 1 cycle. By the performance of this in-situ temperature-dependent measurement, the elastic component of Cu protrusion was determined to be 0.4 μm.

The profile of H_{avg} can be divided into 3 stages, A, B, and C based on its slope (Fig. 5). Stage A is from RT to about 250 °C. In this stage, the copper remained within the hole. Because of the constraint of the surrounding glass substrate and the adhesion force at the copper-glass interface, H_{avg} increased relatively slowly. When the temperature reached 250 °C, H_{avg} was about 0 μm, which meant copper started to protrude from the glass substrate (stage B). In stage B, which lasts until 400 °C, H_{avg} increased significantly faster compared with stage A, which was caused by the plastic deformation and creep of the copper at elevated temperature once the copper vias extended past the glass. Additionally, the upper portion of the copper was free from the interfacial adhesion force and the constraint of the glass substrate, which accelerated the growth of the copper protrusion height. In stage C, the TGV sample was cooled from 400 °C to RT. The irreversible copper protrusion was about 1.3 μm after one thermal cycle because of the plastic deformation and the creep of the copper. Similarly, the copper protrusion of another four samples with different ramp rates (50C/min, 30C/min, 15C/min, and 4C/min) were measured to study the effect of the ramp rate on the copper protrusion (Fig. 6). The results show that the copper protrusion height increases significantly with a slower ramp rate, because more significant creep and plastic deformation occur in the copper during the thermal cycling with slower ramp rate. A subsequent polishing can remove the copper protrusion to avoid a reliability issue at the back-end-of-line (BEOL) structure.

Moreover, the copper protrusion was measured at low temperatures. A TGV sample was cooled from RT to −40 °C with a ramp rate 50 °C/min and reheated to RT. The copper behaved elastically, and no irreversible protrusion was observed, therefore, H_{avg} changed linearly with the temperature (Fig. 7).

3.2. *In-plane deformation of glass*

Large thermomechanical stresses develop at the copper-glass interface because of the significant CTE mismatch between the copper and

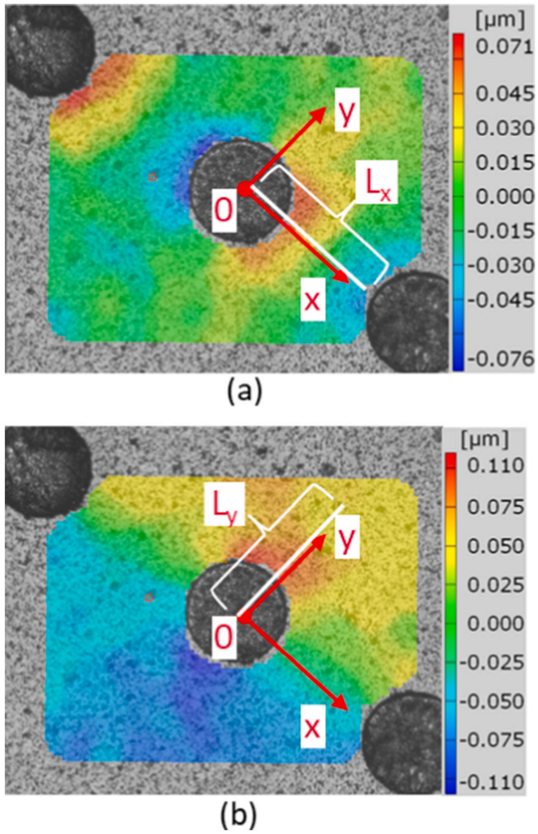

Fig. 8. (a) D_x of glass displacement at 250 °C; (b) D_y of glass displacement at 250 °C.

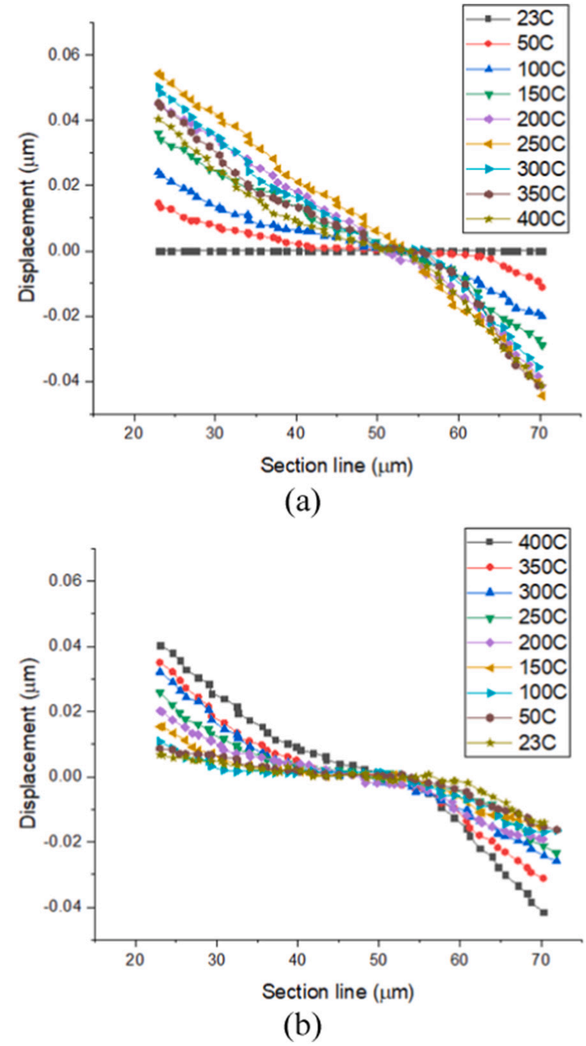

Fig. 9. (a) D_x gradient on section line L_x during heating; (b) D_x gradient on section line L_x during cooling.

glass, which can lead to various reliability issues at elevated temperatures. In this work, the 2D DIC technique was employed to analyze the in-plane deformation of the glass during thermal cycling. Based on the results, an in-depth understanding of the interaction between a copper via and the surrounding glass at elevated temperatures can be attained. The measurement FOV was set to 220 × 200 μm. Three vias can be inspected in the FOV so that the orientation (pitch x and pitch y) of the TGV sample can be identified. The measurement temperature profile was set from RT to 400 °C and then cooled to RT. Four different temperature ramp rates (4 °C/min, 15 °C/min, 30 °C/min, 50 °C/min) were tested to address the ramp rate effect on the results. A full field of in-plane displacements of the glass at different temperatures was captured by the 2D DIC system. As an example, Fig. 8 shows the displacement results of the glass near the copper via in x (Fig. 8a) and y (Fig. 8b) direction at 250 °C during heating with a ramp rate of 50 °C/min. A local Cartesian coordinate system was defined in the displacement field with the origin located in the center of the copper via. The x axis is in the direction of pitch x, and the y axis is in the direction of pitch y. Fig. 8(a) shows the x component (D_x) of the glass in-plane displacement with a maximum value about 71 nm. Because of the effect of the neighboring via in pitch-x direction, the resultant thermal stresses canceled out, leading to the 0 displacement of the glass at the middle area between two nearby copper vias. Similarly, the glass in-plane displacement in the y direction (D_y) had the largest value of 115 nm near the edge of the copper via (Fig. 8b). However, the effect of the neighboring vias in the y direction was negligible because pitch y was too large, thus, D_y was larger than D_x.

White section lines L_x and L_y were defined in the glass displacement contour (Fig. 8). L_x and L_y are each 70 μm long, as measured from the origin. D_x on section line L_x at different temperatures during heating and cooling was plotted in Fig. 9 for quantitative analysis. At each temperature, D_x on the section line L_x decreases as the distance from the edge of the copper via increases, and D_x reduces to 0 when it is 55 μm away from the center of the copper via, which is exactly the middle area between two copper vias. In the same manner, D_y on section line L_y at different temperatures during heating and cooling was plotted in Fig. 10. Because the effect of neighboring copper vias in the y direction was negligible, D_y does not decrease as fast as D_x at each temperature, and D_y had a relatively larger magnitude than D_x.

A 4 × 4 μm square area, referred as "area A", was defined on the in-plane displacement contour near the edge of copper via in the x direction (Fig. 11). Area A was the most critical region under the largest compression and tensile force during heating and cooling. A TGV samples were heated from RT to 400 °C and then cooled to RT with the same ramp rate. Four ramp rates (4 °C/min, 15 °C/min, 30 °C/min, 50 °C/min) were applied to investigate the strain rate dependent copper behavior. An average D_x of area A in the 4 TGV samples was plotted over temperatures (Fig. 12). The displacement results show that Dx increased as the TGV sample was heated from RT to 250 °C, which indicated that the glass was pushed toward the positive x axis direction because of the expansion of the copper. However, when the temperature passed 250 °C, D_x started to decrease. That was attributed to the protrusion of the copper, which reduced the volume of the copper in the glass. Moreover, the plastic deformation and creep of the copper at elevated temperatures caused a reduction of the thermal stress at the copper-glass interface, which contributed to the decrease of the D_x. The temperature ramp rate

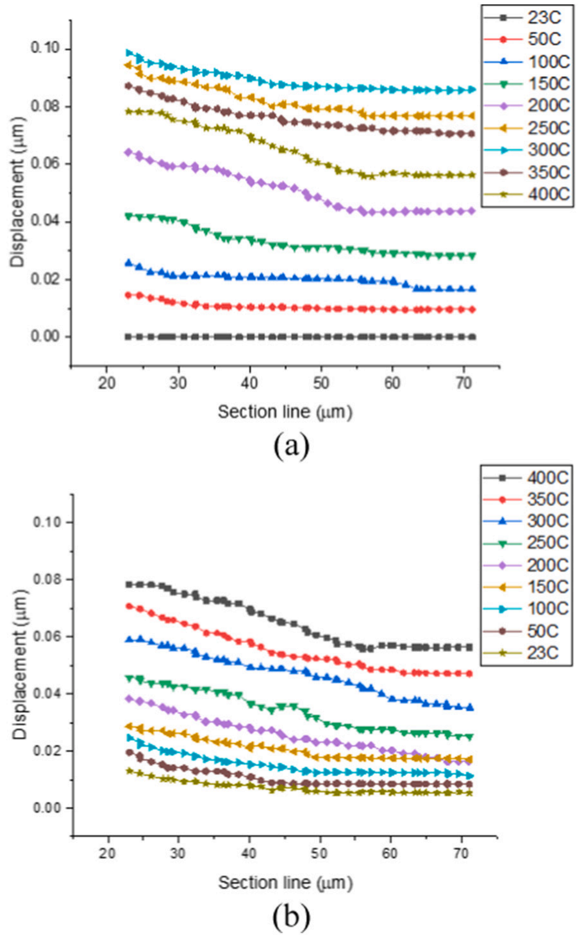

Fig. 10. (a) D_y gradient on section line L_y during heating; (b) D_y gradient on section line L_y during cooling.

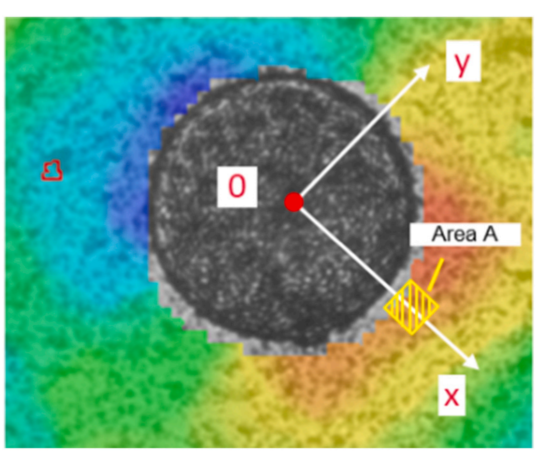

Fig. 11. A 4 × 4 μm area A defined on the displacement contour near the edge of the copper via.

shows a great impact on the in-plane displacement of the glass. Utilizing a slower ramp rate is an effective way to alleviate the in-plane deformation of the glass, because the slower ramp rate provides longer duration at high temperature so that the copper can creep more.

The peak glass displacements of ramp rate 50 °C/min, 30 °C/min, 15 °C/min and 4 °C/min were about 75 nm, 67 nm, 65 nm, and 42 nm, respectively. As the TGV samples were cooled from 400 °C to RT, D_x decreased gradually. And the sample with ramp rate 4 °C/min had the

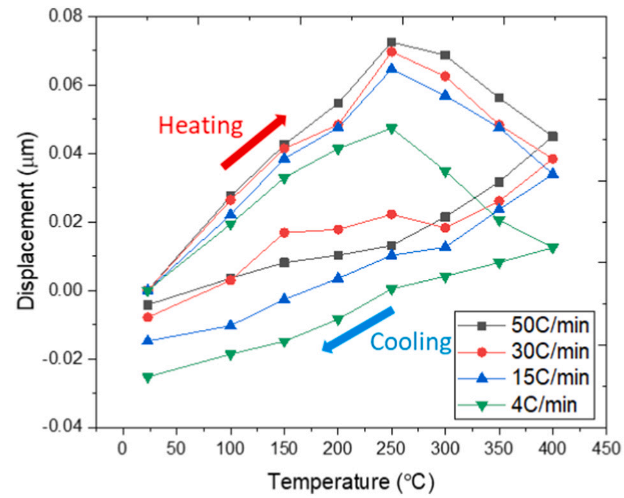

Fig. 12. Average D_x of the area A near the edge of copper via.

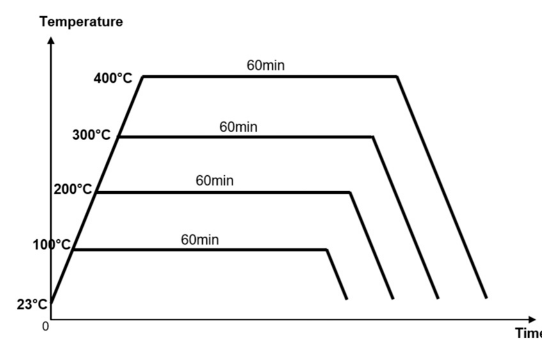

Fig. 13. Temperature profile for copper via stress relaxation test.

largest displacement in the negative x axis direction because of the pulling force from copper during cooling. Slower ramp rate resulted in longer exposure to elevated temperatures, which would cause larger volume of copper to protrude from the glass because of the creep of copper. Therefore, the glass near the edge of the copper vias was pulled more in the negative x axis direction.

The presented findings in Fig. 12 agrees with recent publication [9–11] that showed that during heating that the formation of radial crack was dependent on the applied heating rate, as higher heating rates led to increased crack probability. They found that when slower heating rates of ≤6.5 °C/min was used, no cracks were formed around the Cu TGV. This indicates the activation of sufficient stress relaxation in the copper, leading to reduced substrate stress, preventing the formation of radial cracks.

3.3. Copper via stress relaxation

The temperature and the temperature duration are important factors in the annealing process. Proper annealing temperature with reasonable duration can improve the material properties of the copper via and assure manufacturing efficiency. The stress relaxation tests of the copper via were conducted to investigate the temperature and duration-dependent copper thermomechanical behavior and glass in-plane displacement. Four TGV samples were tested individually at peak temperature of 100 °C, 200 °C, 300 °C, 400 °C. The temperatures ramped up at a rate of 15 °C/min until the hotplate reached the peak and held there for 60 min. Each sample was cooled at the same ramp rate until reaching RT. Fig. 13 illustrates the times and temperatures used in the tests.

The D_x of area A in the four samples were measured and plotted in

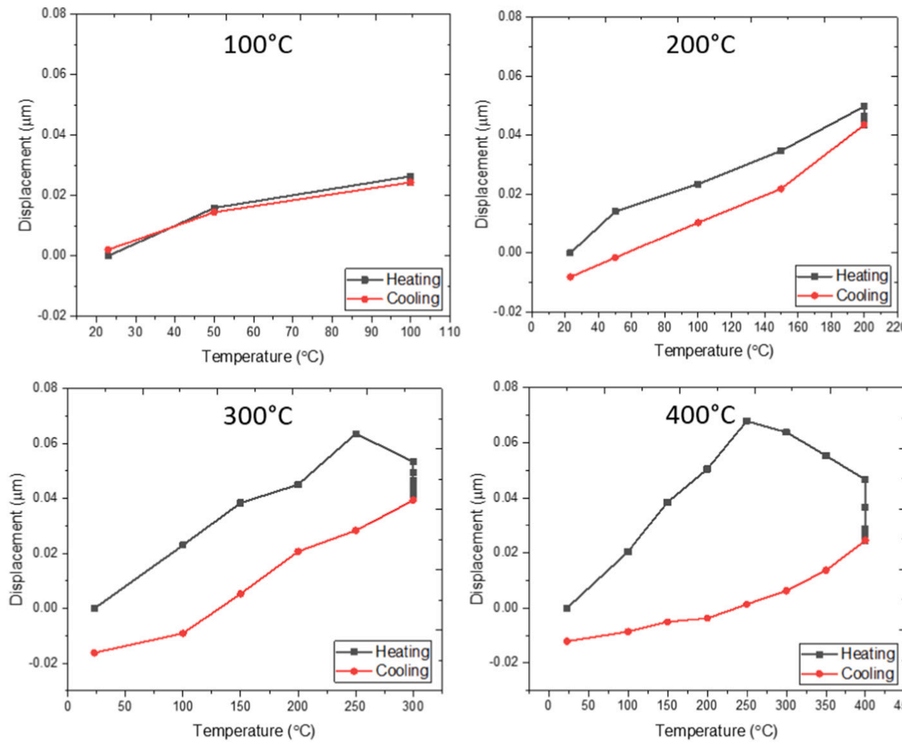

Fig. 14. Dx of area A in TGV samples during stress relaxation test, four different TGV samples were tested at 100 °C, 200 °C, 300 °C, 400 °C, respectively.

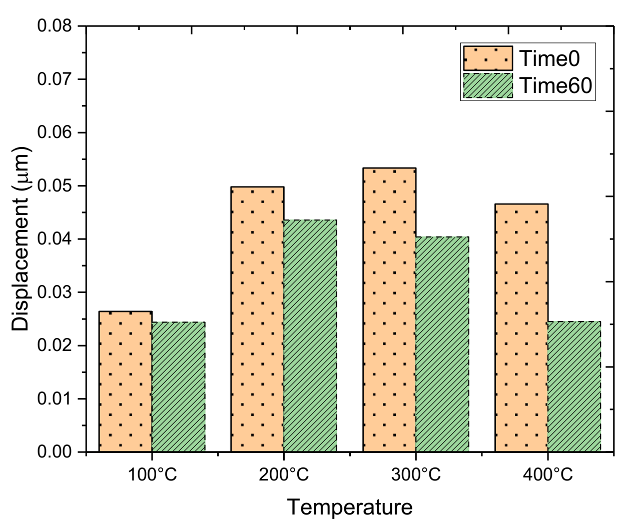

Fig. 15. D_x of area A at different target temperatures, D_x at the beginning of the duration is represented by Time0, Dx at the end of the duration is represented by Time60.

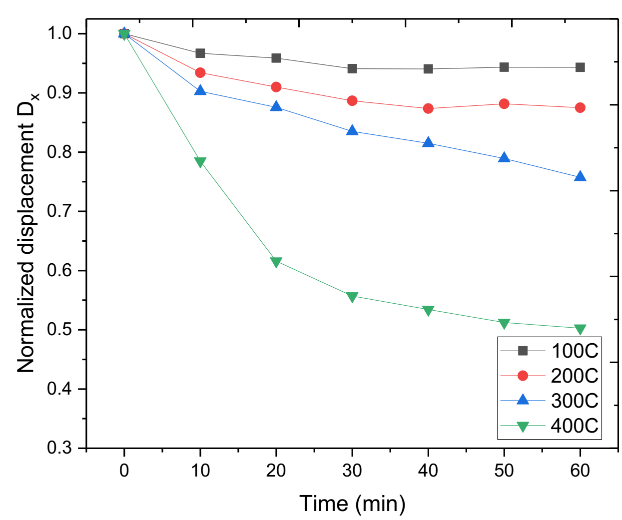

Fig. 16. Dx of area A in TGV samples during stress relaxation at 100 °C, 200 °C, 300 °C, 400 °C for 60 min.

Fig. 14. The data point of D_x was measured every 50 °C from RT to the target temperature. After the peak temperature was reached, Dx was measured every 10 min until 60 min passed. Fig. 14 shows the profile of D_x during the tests with different peak temperatures. During the duration at the peak temperature, D_x decreased gradually because of creep of the copper. The reduction of the D_x during the 60 min at 100 °C, 200 °C, 300 °C, and 400 °C was about 2 nm, 6 nm, 13 nm, and 22 nm, respectively (Fig. 15). The normalized D_x in the duration is plotted in Fig. 16. The results show that the copper via has more significant creep at higher temperatures. Therefore, a relatively higher temperature is preferred in the TGV annealing process to improve the material properties of the copper. This study can be used as a good reference in TGV manufacturing to justify an appropriate annealing temperature profile.

4. Numerical simulation and discussion

Numerical simulation was performed to have a more comprehensive understanding of the interaction between the copper via and the glass during thermal cycling. The model was created in Ansys Workbench. Nonlinear mechanical mesh type is selected to reflect the nonlinear properties of the copper at high temperatures. In this model, the TGV sample is heated from RT to 400 °C with different ramp rates. Several assumptions are made to simplify the model.

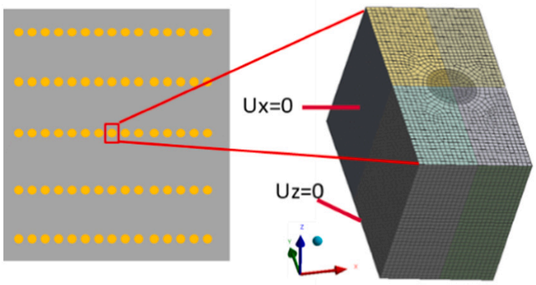

Fig. 17. The finite element model of TGV with one copper via.

Table 1
The material properties in the model.

	CTE (ppm/°C)	Young's modulus (GPa)	Poisson's ratio	Ref.
Copper	17	127	0.34	[12]
Glass	0.5	70	0.16	[12]

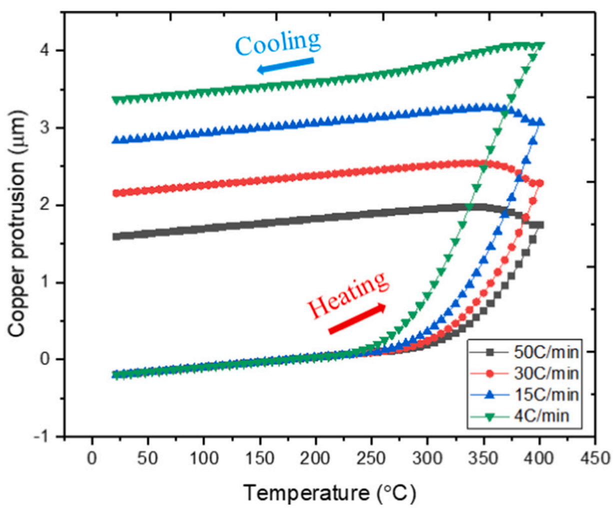

Fig. 18. The copper protrusion results with different ramp rate based on the simulation.

1. The effect of adjacent copper vias in x direction is considered, thereby the two side faces do not have displacement in x direction (x = 0, Fig. 17). While the effect of adjacent copper vias in y direction is ignored, because the pitch y of the copper vias is much larger than pitch x.
2. The measured TGV samples are symmetrical and the interested copper via is exactly at the middle of the TGV sample, so the model of the TGV can be simplified to be a single via model. It is a half model, because the TGV samples are symmetric about the middle plane in the thickness direction, thereby the bottom face does not have displacement in z direction (z = 0, Fig. 16).
3. The copper via and the glass share a perfectly bonded interface, and the copper is uniformly distributed in the via without any voids.

The material properties of copper and glass in this model are listed in Table 1. The copper was considered as a nonlinear material and the creep model (Eq. (1)) [33] was adopted in this simulation. The initial material constants C1, C2, and C4 are referred from De Messemaeker et al. study [22]. However, to achieve better correlation between the experiment and simulation results, the time hardening creep model was applied which includes the time effect (C3). And the material constants were adopted from Messemaeker's work and then optimized. The

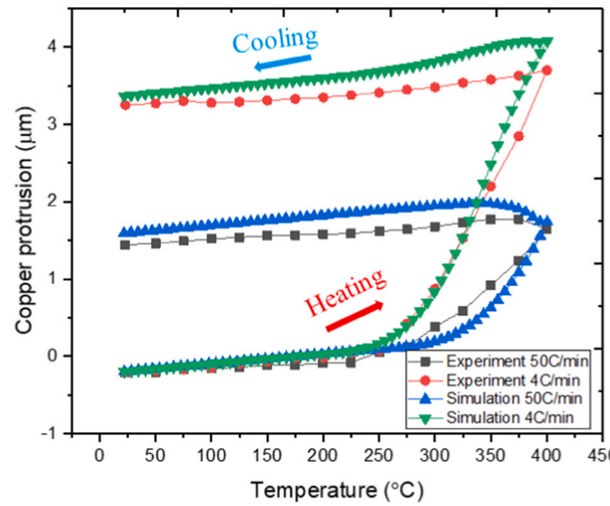

Fig. 19. The copper protrusion results.

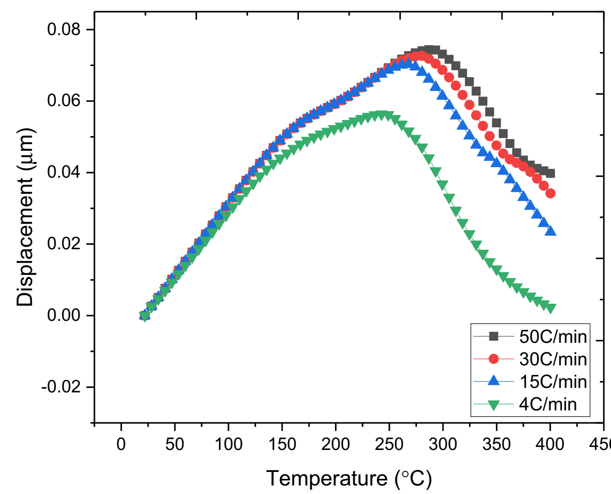

Fig. 20. The in-plane displacement of the glass at different ramp rates during heating from the numerical model.

material constant optimization process was done based on the experimental and simulation results of the copper protrusion height. There are in total 32 data points in the copper protrusion measurement during temperature cycling. The offsets between the experiment and simulation results of the 32 data points were summed up to assess the correlation. Based on the simulation results with different combinations of C_1, C_2, C_3, and C_4, the material constants C_1, C_2, C_3, and C_4 were determined to be 40, 1.8, 0.3, and 13,500, respectively.

$$\dot{\varepsilon}cr = c1\sigma^{C2}t^{c3}e^{-c4/T} \quad (1)$$

where ε_{cr} is the creep strain rate (1/s), σ is stress (MPa), t is time (sec), and T is the temperature (K).

Based on the numerical model, the copper protrusion results during thermal cycling with different ramp rates are simulated (Fig. 18). The results that the copper protrusion height increases considerably as the ramp rate decreases, which agrees with the results from the in-plane deformation measurement of the glass. Because of the more significant creep and plastic deformation of the copper during the thermal cycling with slower ramp rate, the copper tends to have higher protrusion, meanwhile, the in-plane deformation of the glass decreases as a result of the copper volume reduction in the glass. To validate the results from the numerical model, the copper protrusion results from the fastest ramp

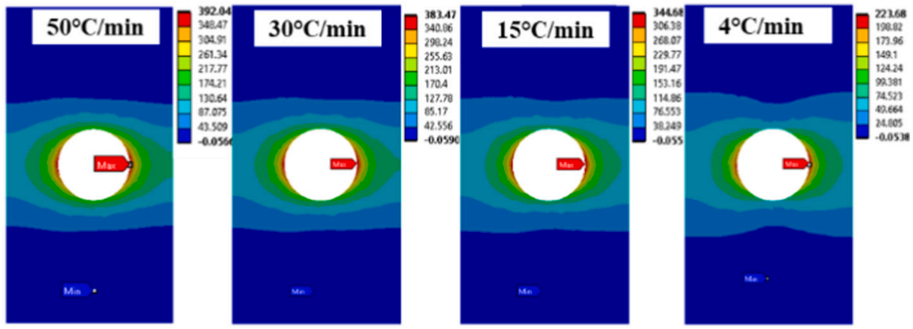

Fig. 21. The max. principal stress on the top surface of the glass at 250 °C during thermal cycling.

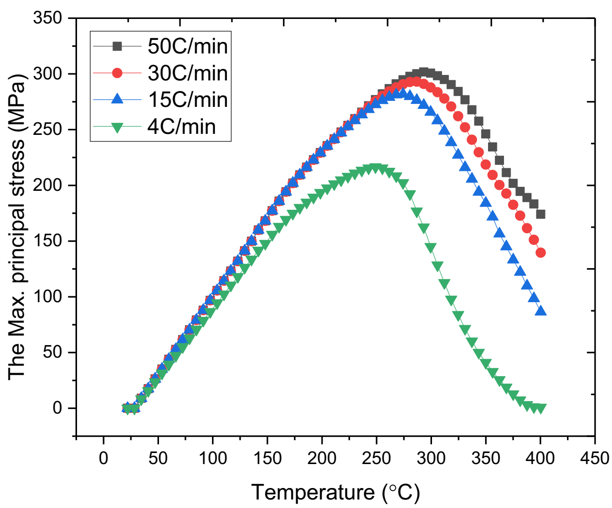

Fig. 22. The max. principal stress of the glass top surface during heating from the numerical model.

rate (50 °C/min) and the slowest ramp rate (4 °C/min) are selected and plotted in Fig. 19, which show good agreement.

Based on the numerical model, the maximum in-plane displacements (D_x) of the glass with different ramp rates are presented in Fig. 20. The results show that D_x reaches its maximum at around 250 °C, and the maximum D_x can be reduced with a slower temperature ramp rate. Because of more significant plastic deformation and creep of the copper during slower ramp rates, the thermal stress near the copper-glass interface was reduced. Fig. 21 shows the max. principal stress of the glass top surface with different ramp rates. The glass near the edge of the copper-glass interface in the pitch x direction are the most critical region under the largest stress. In Fig. 22, the max. principal stresses of the glass top surface reaches its maximum at around 250 °C then it starts to decrease, which correlates with the in-plane displacement results (Fig. 20). As for the entire glass substrate, the max. principal stress has the largest value at the middle of the copper-glass interface (Fig. 23). The max. principal stress of the entire glass and the glass top surface exhibit a similar trend, but the transition temperatures when the max. principal stresses start to decrease are different for the glass top surface (250 °C – 300 °C) and the entire glass (325 °C – 375 °C). It is because that the max. principal stress of the glass top surface is affected by the protrusion of the copper which causes copper volume reduction within the

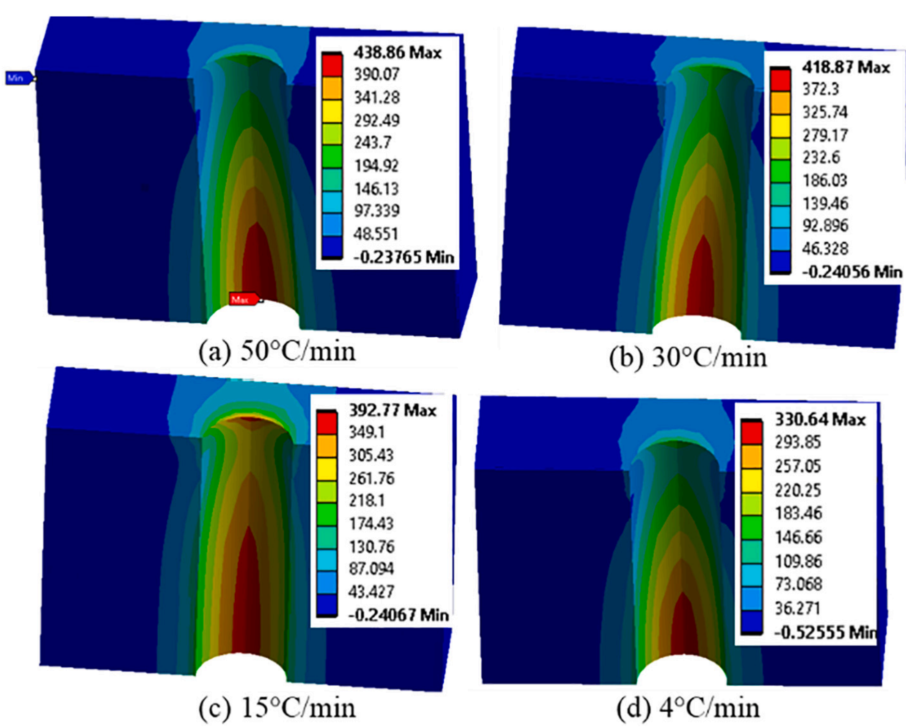

Fig. 23. The cross-section view of the max. principal stress on the entire glass during thermal cycling.

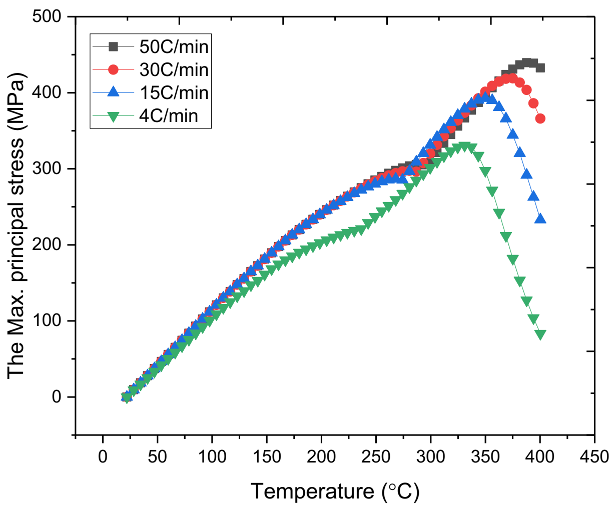

Fig. 24. The max. principal stress of the entire glass during heating from the numerical model.

glass, thus, the max. principal stress decreases. However, the max. principal stress of the entire glass occurs at the center of the copper-glass interface where the copper protrusion has a negligible effect. Therefore, the max. principal stress of the entire glass has a larger value and a high transition temperature (Fig. 24).

5. Conclusion

In this study, the copper protrusion of TGV sample in the thermal cycling was investigated. Irreversible copper protrusion was observed after thermal cycling, which was caused by the plastic deformation and creep of copper at elevated temperatures. While the copper via behaved elastically at low temperature range from RT to −40 °C. In-plane displacement of glass in TGV sample during thermal cycling was measured using 2D DIC system. The displacement of the glass increased with the temperature from RT to 250 °C, then it started to decrease because of the copper protrusion and creep at elevated temperatures. It was found that the neighboring copper via with smaller pitch had great impact on the displacement results. Glass near the edge of copper via had the largest in-plane displacement because of the thermal stress at the copper-glass interface. The copper tended to be annealed sufficiently at elevated temperature with slower ramp rate and reasonable long duration, which could help reducing the thermal stress at the copper-glass interface and minimizing the in-plane deformation of the glass. Based on the simulation results, the glass at the middle of the copper-glass interface and near the edge of the copper via is the most critical region.

Declaration of competing interest

The authors declare that they have no known competing financial interests or personal relationships that could have appeared to influence the work reported in this paper.

Acknowledgements

The authors acknowledge Corning Research and Development Corporation for the support of this work.

CRediT authorship contribution statement

Ke Pan is the main person conducting the experimental work and numerical simulation. He developed the overall approach for the experiments. Jiefeng Xu built the numerical model. Yangyang Lai helped with performing the measurement. Seungbae Park is the advisor of this study, and he provided many useful suggestions for the project. Chukwudi Okoro, Dhananjay Joshi and Scott Pollard provided the samples for the experiments, and they guided the overall workflow of this experiment and simulation work. All authors read and approved the revised manuscript.

References

[1] J.Y. Lee, S.W. Lee, S.K. Lee, J.H. Park, Through-glass copper via using the glass reflow and seedless electroplating processes for wafer-level RF MEMS packaging, J. Micromech. Microeng. 23 (8) (2013).
[2] H. Wang, et al., Product level design optimization for 2.5D package pad cratering reliability during drop impact, Proc. Electron. Components Technol. Conf. 2019 (May) (2019) 2343–2348.
[3] K. Pan, J.H. Ha, H.Y. Wang, V. Veeraraghavan, S.B. Park, The effect of solder paste volume on surface mount assembly self-alignment, Procedia Manuf. 38 (2019) (2019) 1381–1393.
[4] S. Takahashi, et al., Development of through glass via technology for 3D packaging, in: EMPC 2013 - Eur. Microelectron. Packag. Conf. Wind. Roads Electron. Packag, 2013, pp. 1–5.
[5] O. Ahmed, G. Jalilvand, S. Pollard, C. Okoro, T. Jiang, The interfacial reliability of through-glass vias for 2.5D integrated circuits, Microelectron. Int. 37 (4) (2020) 181–188.
[6] J. Cheng, et al., Performance and Process Comparison Between Glass and Si Interposer for 3D-IC Integration Keywords, no. Imaps, 2013, pp. 618–624.
[7] S. Kuramochi, H. Kudo, M. Akazawa, H. Mawatari, Glass interposer technology advances for high density packaging, in: IEEE CPMT Symposium Japan (ICSJ), 2016, pp. 2–5.
[8] M. Töpper, et al., 3-D thin film interposer based on TGV (through glass vias): an alternative to Si-interposer, Proc. - Electron. Components Technol. Conf. (2010) 66–73 (no. Table 1).
[9] C. Okoro, P. Maurey, S. Pollard, Time and temperature dependence of copper protrusion in metallized through-glass vias (TGVs) fabricated in fused silica substrate, IEEE Trans. Device Mater. Reliab. 21 (1) (Mar. 2021) 129–136.
[10] C. Okoro, S. Jayaraman, S. Pollard, Understanding and eliminating thermo-mechanically induced radial cracks in fully metallized through-glass via (TGV) substrates, Microelectron. Reliab. 120 (May 2021), 114092.
[11] C. Okoro, A. Park, T. Allowatt, S. Pollard, Elimination of Thermo-mechanically driven circumferential crack formation in copper, IEEE Trans. Device Mater. Reliab. 21 (3) (2021) 354–360.
[12] W. Zhang, S.Y. Li, Z.X. Yang, Y. Mao, S.Y. Xu, Microstructure evolution and mechanical properties of copper bonding wire during continuous annealing, Mater. Res. Innov. 19 (March) (2015) S225–S229.
[13] H. Zhang, Z. Guo, Thickness dependence and anisotropy of capped diamond thermal conductivity on cooling of pulse-operated GaN HEMTs, IEEE Trans. Components, Packag. Manuf. Technol. 11 (2) (2021) 233–240.
[14] J. Yang, J. Xu, S. Park, Identification of polymer materials in electronic packages including counterfeit prevention, Proc. Electron. Components Technol. Conf. 2020 (June) (2020) 2317–2324.
[15] C. Okoro, P. Maurey, S. Pollard, Time and temperature dependence of copper protrusion in metallized through-glass vias (TGVs) fabricated in fused silica substrate, IEEE Trans. Device Mater. Reliab. 21 (1) (2021) 129–136.
[16] P. Saettler, M. Boettcher, K. Wolter, Characterization of the Annealing Behavior for Copper-filled TSVs, 2012, pp. 619–624.
[17] D. Zhang, K. Hummler, L. Smith, J.J.Q. Lu, Backside TSV protrusion induced by thermal shock and thermal cycling, Proc. Electron. Components Technol. Conf. (2013) 1407–1413.
[18] C. Gregory, et al., Characterization of Thermo-mechanical stress and reliability issues for cu-filled TSVs, Proc. Electron. Components Technol. Conf. (2011) 1815–1821.
[19] A. Heryanto, et al., Effect of copper TSV annealing on via protrusion for TSV wafer fabrication, J. Electron. Mater. 41 (9) (2012) 2533–2542.
[20] C. Okoro, et al., Elimination of the axial deformation problem of cu-TSV in 3D integration, AIP Conf. Proc. 1300 (2010) 214–220.
[21] K. Pan, et al., Investigation of copper and glass interaction in through glass via (TGV) during thermal cycling, Proc. Electron. Components Technol. Conf. (2021) 1660–1666.
[22] J. De Messemaeker, et al., Impact of post-plating anneal and through-silicon via dimensions on cu pumping, Proc. Electron. Components Technol. Conf. (2013) 586–591.
[23] N. Ranganathan, K. Prasad, N. Balasubramanian, K.L. Pey, A study of thermo-mechanical stress and its impact on through-silicon vias, J. Micromech. Microeng. 18 (7) (2008).
[24] X. Liu, Q. Chen, P. Dixit, R. Chatterjee, R.R. Tummala, S.K. Sitaraman, Failure mechanisms and optimum design for electroplated copper through-silicon vias (TSV), Proc. Electron. Components Technol. Conf. (2009) 624–629.
[25] T. Huang, V. Sundaram, P.M. Raj, H. Sharma, R. Tummala, Adhesion and reliability of direct cu metallization of through-package vias in glass interposers, Proc. Electron. Components Technol. Conf. (2014) 2266–2270.
[26] P. Kumar, I. Dutta, M.S. Bakir, Interfacial effects during thermal cycling of cu-filled through-silicon vias (TSV), J. Electron. Mater. 41 (2) (2012) 322–335.

[27] S.K. Ryu, K.H. Lu, X. Zhang, J.H. Im, P.S. Ho, R. Huang, Impact of near-surface thermal stresses on interfacial reliability of through-silicon vias for 3-D interconnects, IEEE Trans. Device Mater. Reliab. 11 (1) (2011) 35–43.
[28] K. Demir, A. Armutlulu, V. Sundaram, P.M. Raj, R.R. Tummala, Reliability of copper through-package vias in bare glass interposers, IEEE Trans. Components Packag. Manuf. Technol. 7 (6) (2017) 829–837.
[29] G. Jalilvand, O. Ahmed, N. Dube, T. Jiang, Study of the impact of pitch distance on the statistical variation of TSV protrusion and the underlying mechanisms, Proc. Electron. Components Technol. Conf. 2020-June (2020) 1173–1179.
[30] C. Cai, K. Pan, J. Yang, S. Park, Comparative analysis of package warpage using confocal method and digital image correlation, Intersoc. Conf. Therm. Thermomech. Phenom. Electron. Syst. ITHERM 2020 (July) (2020) 945–949.
[31] V. Pham, J. Xu, K. Pan, J. Wang, S. Park, H. Wang, Investigation of underfilling BGAs packages – thermal fatigue, Proc. Electron. Components Technol. Conf. (2020) 2252–2258.
[32] K. Pan, J.H. Ha, H. Wang, J. Xu, S. Park, An analysis of solder joint formation and self-alignment of chip capacitors, IEEE Trans. Components Packag. Manuf. Technol. 11 (1) (2021) 161–168.
[33] F.A. Cozzarelli, R.P. Shaw, A combined strain and time-hardening non-linear creep law, Int. J. Nonlinear Mech. 7 (2) (1972) 221–234.